

# Vectorcardiographic loop alignment for fetal movement detection using the Expectation-Maximization algorithm and Support Vector Machines

R. Vullings, M. Mischi

**Abstract**—Reduced fetal movement is an important parameter to assess fetal distress. Currently, no suitable methods are available that can objectively assess fetal movement during pregnancy. Fetal vectorcardiographic (VCG) loop alignment could be such a method. In general, the goal of VCG loop alignment is to correct for motion-induced changes in the VCGs of (multiple) consecutive heartbeats. However, the parameters used for loop alignment also provide information to assess fetal movement. Unfortunately, current methods for VCG loop alignment are not robust against low-quality VCG signals. In this paper, a more robust method for VCG loop alignment is developed that includes a priori information on the loop alignment, yielding a maximum a posteriori loop alignment. Classification, based on movement parameters extracted from the alignment, is subsequently performed using support vector machines, resulting in correct classification of (absence of) fetal movement in about 75% of cases. After additional validation and optimization, this method can possibly be employed for continuous fetal movement monitoring.

## I. INTRODUCTION

The vectorcardiogram is a 3-dimensional representation of the electrical activity of a beating heart and as such holds more diagnostic information than its 1-dimensional counterpart, the electrocardiogram. The alignment of vectorcardiographic (VCG) loops is of interest in electrocardiographic (ECG) applications where more than one heartbeat is analyzed at the same time. However, mechanical movement of the heart, e.g. induced by respiration, causes variations in the ECG morphology, complicating diagnostics on electrical instability.

In the literature [1], [2], methods have been proposed for spatiotemporal alignment of VCG loops to minimize movement-induced ECG variability. These methods operate by applying a set of transformations – time synchronization, rotation, and scaling – on each VCG loop to maximize the correspondence with a reference VCG loop. However, VCG loop alignment does not only have value in facilitating assessment of multiple heartbeats simultaneously, but, based on the applied transformations, also information on mechanical movement of the heart can be obtained.

In the case of fetal ECG measurements on the maternal abdomen, the mechanical movement of the heart would not only entail movement of the fetal heart inside the fetal thorax, but would mostly entail movement of the fetal thorax with respect to the electrode grid on the maternal abdomen. In other words, fetal VCG loop alignment would yield a tool to monitor fetal movement. Such movement has been proven

to be a valuable diagnostic parameter to assess fetal distress [3] and is currently mostly assessed by maternal perception, which is liable to substantial inter-patient variability [4].

Two problems arise aiming at the use of fetal VCG loop alignment for fetal movement detection. Firstly, the signal quality of abdominal fetal ECG measurements is much poorer than that of adult ECG recordings. In [5], it has been reported that the performance of the earlier-mentioned VCG loop alignment methods deteriorates with decreasing signal-to-noise ratios. The robustness of VCG loop alignment, hence, needs to be improved. Secondly, the transformations applied in the loop alignment do not provide direct information on fetal motility. Therefore, these transformations need to be used as input in a classification (i.e. between fetal movement and fetal rest) problem.

In this paper, the first problem is addressed by extending the maximum-likelihood (ML) approach of the existing methods to a maximum-a-posteriori (MAP) approach, in which prior assumptions on the transformations are included to increase the robustness of the alignment. The parameter inference problem for this MAP approach is solved using the expectation-maximization (EM) algorithm. The second problem is addressed by using support vector machines (SVM) to achieve correct classification of episodes of fetal movement and fetal rest.

## II. VECTORCARDIOGRAPHIC MOVEMENT ASSESSMENT

### A. Vectorcardiographic loop alignment

In the model proposed in [2], the VCG loop at time  $t$  can be described by a  $[3 \times M]$  matrix  $Z_t$ , where  $M$  is the length of the VCG loop. Each of the three  $[1 \times M]$  row vectors in  $Z_t$  constitutes the QRS-part of one of the three orthogonal Frank leads.

Based on the quasi-periodicity of the ECG (and also of the derived VCG),  $Z_t$  can be described as a function of the preceding VCG loop  $Z_{t-1}$ . In this description,  $Z_{t-1}$  is altered by a series of transformations, i.e., time-synchronization, scaling, and rotation [2]. Mathematically, the relation between  $Z_t$  and  $Z_{t-1}$  can be described as

$$Z_t = RBZ_{t-1}J_\tau + H. \quad (1)$$

Here,  $R$  is a  $[3 \times 3]$  rotation matrix and  $B$  is a  $[3 \times 3]$  diagonal scaling matrix.  $J_\tau$  indicates the shift matrix that shifts  $Z_{t-1}$  over  $\tau$  samples. Finally,  $Z_t$  is assumed to be additively corrupted by a  $[3 \times M]$  zero-mean Gaussian noise matrix  $H$  that accounts for any aspect of  $Z_t$  that cannot be described by the transformation of  $Z_{t-1}$ .

R. Vullings and M. Mischi are with the Faculty of Electrical Engineering, Eindhoven University of Technology, Eindhoven, The Netherlands  
r.vullings@tue.nl

Let us initially assume the time shift  $\tau$  to be constant and known. Inference of the model parameters hence reduces to finding the MAP estimates of  $R$  and  $B$ . Using Bayes' rule, the posterior probability distribution for these parameters, given the recorded VCG loops  $Z_t$  and  $Z_{t-1}$ , and the time shift  $\tau$ , can be written as:

$$p(R, B | Z_t, Z_{t-1}, \tau) \propto p(Z_t | R, B, Z_{t-1}, \tau) p(R, B). \quad (2)$$

In order to maximize the posterior probability distribution  $p(R, B | Z_t, Z_{t-1}, \tau)$  for both  $R$  and  $B$ , we reformulate our inference problem to first find the MAP estimate for  $B$ , given the measurement data  $Z_t$  and  $Z_{t-1}$ , and a hidden nuisance parameter  $R$  [6]. The estimation of  $B$  now boils down to application of the EM algorithm.

In order to infer  $B$ , we can maximize the posterior probability distribution of  $B$ , while marginalizing Eq. (2) over the hidden parameter  $R$ :

$$\hat{B} = \arg \max_B \int p(Z_t | R, B, Z_{t-1}, \tau) p(R, B) dR. \quad (3)$$

Exploiting the fact that the logarithm is a monotonically increasing function, and introducing the probability distribution  $p(R | Z_t, \hat{B}^{\text{old}})$  in which  $\hat{B}^{\text{old}}$  is defined as an initial guess for  $\hat{B}$ , Eq. (3) can be re-expressed as:

$$\hat{B} = \arg \max_B \ln \int p(R | Z_t, \hat{B}^{\text{old}}) \frac{p(Z_t | R, B) p(R, B)}{p(R | Z_t, \hat{B}^{\text{old}})} dR. \quad (4)$$

Here, for clarity, the terms  $Z_{t-1}$  and  $\tau$  have been omitted.

Using Jensen's inequality, we can define a lower bound  $\mathcal{L}$  for the term on the righthand-side of Eq. (4):

$$\mathcal{L} = \int p(R | Z_t, \hat{B}^{\text{old}}) \ln \frac{p(Z_t | R, B) p(R, B)}{p(R | Z_t, \hat{B}^{\text{old}})} dR. \quad (5)$$

With this lower bound, we have transformed the logarithm of an integral in Eq. (4) into the integral of a logarithm in Eq. (5). By iteratively maximizing  $\mathcal{L}$  with respect to  $B$  (referred to as the *M-step*) and subsequently updating  $\mathcal{L}$  for the new  $\hat{B}^{\text{old}}$  (referred to as the *E-step*), we can ensure that the estimate for  $B$  converges to a local maximum.

1) *E-step: probability distribution of R*: Updating the lower bound, based on the estimate  $\hat{B}^{\text{old}}$ , basically corresponds to updating the probability distribution  $p(R | Z_t, \hat{B}^{\text{old}})$  [6]. This probability distribution can be calculated using Bayes' rule and the model of Eq. (1). Unfortunately, when using this probability distribution in the M-step, an analytically insolvable problem emerges.

To overcome this problem, we assume infinite accuracy in the estimation of  $R$ . As a result, an ML estimate  $R^{\text{ML}}$  can be estimated and used to define the probability distribution  $p(R | Z_t, \hat{B}^{\text{old}})$  as a Dirac function:

$$p(R | Z_t, \hat{B}^{\text{old}}) = \delta(R - \hat{R}^{\text{ML}}). \quad (6)$$

The ML estimate for  $R$  can be calculated following the approach in [2]:

$$\hat{R}^{\text{ML}} = \Theta \Gamma^T, \quad (7)$$

where  $\Theta$  and  $\Gamma$  are the left and right eigenvectors of the matrix  $Z_t J_\tau^T Z_{t-1}^T \hat{B}^{\text{old}T}$ , respectively, and are obtained from the singular value decomposition of this matrix.

2) *M-step: estimation of B*: Combining Eqs. (5)-(7) and omitting terms that do not depend on  $B$ , the lower bound  $\mathcal{L}$  can be written as

$$\mathcal{L} = \ln p(Z_t | \hat{R}^{\text{ML}}, B) + \ln p(\hat{R}^{\text{ML}}, B). \quad (8)$$

The prior probability distribution  $p(\hat{R}^{\text{ML}}, B)$  describes our prior knowledge on scaling and rotation. By assuming these transformations to be statistically independent, and assuming  $\hat{R}^{\text{old}}$  to be known and the scaling to show minor fluctuations between heartbeats [1] (e.g. Gaussian distributed around 1 with variance  $\sigma_B^2$ ), the prior probability distribution can be written as:

$$p(\hat{R}^{\text{ML}}, B) \propto \exp \left[ -\frac{1}{2\sigma_B^2} \|B - I_3\|_F^2 \right], \quad (9)$$

where  $I_3$  is the  $[3 \times 3]$  unit matrix.

Combining Eqs. (8) and (9) and maximizing  $\mathcal{L}$  with respect to  $B$  yields the MAP estimate for  $B$ :

$$\hat{B}_{kk}^{\text{MAP}} = \frac{\sigma_B^2 \left( \hat{R}^{\text{ML}T} Z_t J_\tau^T \hat{Z}_{t-1}^T \right)_{kk} + \sigma_\eta^2}{\sigma_B^2 \left( \hat{Z}_{t-1} J_\tau J_\tau^T \hat{Z}_{t-1}^T \right)_{kk} + \sigma_\eta^2}, \quad (10)$$

where  $X_{kk}$  are the diagonal entries of matrix  $X$  and  $\sigma_\eta^2$  is the variance of the measurement noise. The current estimate  $\hat{B}^{\text{MAP}}$  is used in the next iteration of the EM algorithm as the most recent estimate  $\hat{B}^{\text{old}}$ .

3) *Time synchronization*: Up until now, we have assumed the time shift  $\tau$  to be constant and known. For this constant value of  $\tau$  we can infer both  $\hat{B}$  and  $\hat{R}$ , using the EM algorithm described above. After convergence of the EM algorithm, other values for  $\tau$  can be tested using a grid search. A ML estimate for  $\tau$  can subsequently be inferred according to:

$$\hat{\tau}^{\text{ML}} = \arg \min_\tau \left\| Z_t - \hat{R}^{\text{ML}} \hat{B}^{\text{MAP}} Z_{t-1} J_\tau \right\|_F^2. \quad (11)$$

## B. Movement classification using SVM

As mentioned previously, the transformations applied to the VCG loop  $Z_{t-1}$  to make it resemble  $Z_t$  as much as possible provide information on mechanical movement of the fetal heart. In particular, the rotation matrix  $R$  and the scaling matrix  $B$  provide information on movement. Obviously, when the heart is rotating between beats, this can be seen in the VCG loops as rotation. However, upon rotation of the fetus, the tissue distribution between fetal heart and abdominal electrodes will change as well. This change in tissue distribution affects the volume conductor between heart and electrodes and causes variations in the amplitude of the abdominal fetal ECG, and hence also in the VCG loops.

In this paper, we use two-dimensional SVMs (i.e. SVMs with a two-dimensional data vector) to classify the rotational and scaling information into either fetal movement or fetal rest. In terms of rotation, fetal rest entails a rotation matrix

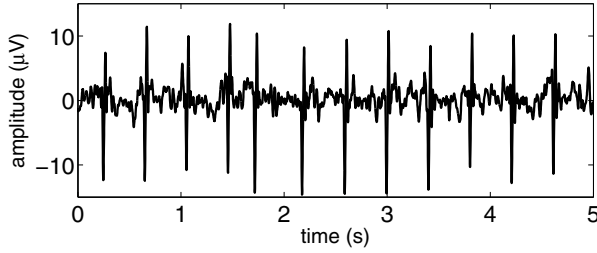


Fig. 1. Example of a fetal ECG recording.

equal to  $I_3$ . Similarly, no scaling with respect to the previous VCG loop entails a unit scaling matrix. The rotational and scaling movement parameters are therefore, respectively, defined as:

$$\mathcal{M}_R = \|\hat{R} - I_3\|_F^2 \quad \text{and} \quad \mathcal{M}_B = \|\hat{B} - I_3\|_F^2, \quad (12)$$

where  $\|\cdot\|_F$  indicates the Frobenius norm.

For the implementation of the SVMs, the standard implementation *svmtrain* in the Bioinformatics toolbox of Matlab<sup>®</sup> (The Mathworks, Inc. Natick, MA) is used. Besides a linear kernel function, the use of quadratic, 3<sup>rd</sup> order polynomial, Gaussian radial basis function (rbf), and 2-layer multilayer perceptron (mlp) kernels is also investigated.

### III. METHODOLOGY FOR EVALUATION

#### A. Data collection

In total, fetal ECG recording has been performed in eight women with gestational ages ranging from 24 to 41 weeks, after having given written informed consent. The ECG recordings have been performed at the Máxima Medical Center (Veldhoven, the Netherlands) with eight electrodes placed on the maternal abdomen. Each recording ranged from 10 to 20 minutes, containing over  $10^4$  fetal heartbeats. The signals have been acquired at 1 kHz sampling rate and have been processed to suppress the maternal ECG and obtain the VCG, using a template subtraction method [7] and Bayesian vectorcardiography method [8], respectively.

In Fig. 1, an example of 5 seconds of data from one of the channels of an 8-channel fetal ECG recording is depicted.

#### B. Definition of $\sigma_\eta$ and $\sigma_B$

In order to implement the VCG loop alignment presented in Section II, the variance of the measurement noise  $\sigma_\eta^2$  and the assumed variance in the scaling  $\sigma_B^2$  need to be defined. Measurement noise is typically temporally uncorrelated with the (quasi-)periodic ECG signal. By averaging various consecutive ECG complexes synchronized on e.g. the QRS complex, a clean reference ECG can hence be obtained. The difference between each individual ECG complex and this reference ECG can subsequently be considered as an approximation of the measurement noise in the individual ECG complexes. In this paper, the value used for  $\sigma_\eta^2$  is the variance of the estimated measurement noise signals, averaged over the eight recorded ECG signals. The optimal value for  $\sigma_B^2$  has empirically been determined at 0.1.

#### C. Reference method for movement detection

Simultaneously with the abdominal fetal ECG measurements, we performed ultrasound recordings using an Aloka SSD1100 ultrasound device (Aloka, Japan). The ultrasound images were stored using a "framegrabber" software for playback options. Fetal movement from the ultrasound recordings was quantified by visual inspection of an expert.

Since fetal movement from VCG loop alignment is determined for every heartbeat, the ultrasound analysis results are resampled to yield a reference classification vector for which the length corresponds to the number of heartbeats.

#### D. Evaluation of SVM

For training the SVMs, various training sets of randomly selected heartbeats are used with the set size ranging from 50 to 2000 heartbeats. The definition of the reference class vector used in the training and classification performance assessment is discussed in Section III-C. To evaluate the performance of the SVMs, the sensitivity and specificity in the detection of fetal movement are determined. The sensitivity is here defined as the fraction of correctly classified heartbeats during fetal movement. The specificity is the fraction of correctly classified heartbeats during fetal rest.

To gauge the performance of the SVMs, their sensitivity and specificity are compared to that of linear classifiers. These linear classifiers are applied with various gradients, ranging from 0.8 to 1.2. For each gradient, virtually all possible biases have been applied, yielding a full ROC curve for the linear classifiers. It has to be stressed that these linear classifiers have been optimized on the basis of the whole data set of the eight abdominal fetal ECG recordings.

### IV. RESULTS OF MOVEMENT DETECTION

In Fig. 2, the fetal movement parameters  $\mathcal{M}_R$  and  $\mathcal{M}_B$  are depicted during periods of fetal movement and fetal rest for one of the fetal ECG recordings. Both  $\mathcal{M}_R$  and  $\mathcal{M}_B$  are significantly different between the two classes (i.e. periods of movement and periods of rest) with p-values smaller than 0.001 for both of them. In Fig. 2(b) and 2(c), VCG loops corresponding to consecutive heartbeats are depicted during a period of low and relatively high fetal motility, respectively.

In Fig. 3, the ROC curves for the linear classifiers are depicted together with the results of the various SVM kernels and sizes of training sets. By performing logistic regression, an optimal gradient and bias for the linear classifiers can be found:  $\mathcal{M}_B = 0.92\mathcal{M}_R - 0.04$ , yielding a sensitivity of 0.47 and specificity of 0.87 (also depicted in Fig. 3 as *log reg*).

### V. DISCUSSION & CONCLUSIONS

In this paper, a method has been presented for MAP alignment of fetal VCG loops with the goal of detecting fetal movement. From the results in Fig. 3, it can be concluded that VCG alignment can be used to classify between fetal movement and fetal rest. The size of the training set used by the SVMs to determine the classifier, seems to have relatively small impact on the specificity of the classification. The classification sensitivity, on average, improves with

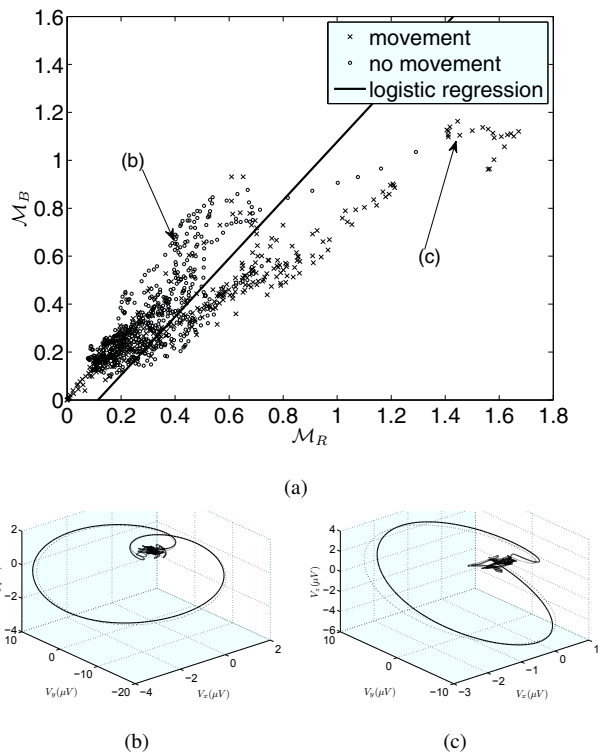


Fig. 2. (a) Fetal movement parameters  $M_R$  and  $M_B$  plotted for one of the fetal ECG recordings, both for periods of fetal movement (indicated with x-marks) and for periods of no fetal movement (indicated with o-marks). The movement/rest periods are determined based on ultrasound analysis. The solid line indicates the optimal linear classification boundary with gradient of  $a = 0.9$ . (b) and (c) Two consecutive VCG loops (solid and dashed lines) during a period of no fetal movement and a period of movement, respectively. The specific fetal movement parameters corresponding to the VCG loops of (b) and (c) are also indicated in (a).

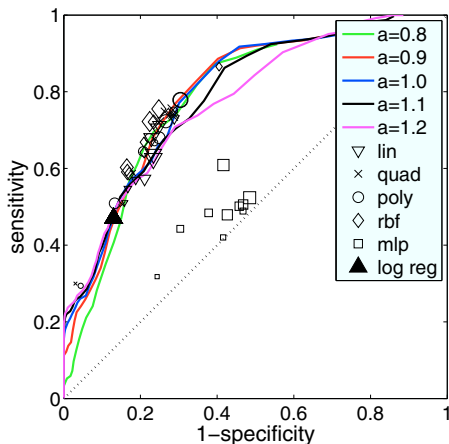


Fig. 3. ROC plot for the fetal movement classification. The lines indicate the classification performance of linear classifiers with a priori defined gradients  $a$ . Each point along the line represents a different bias for the linear classifier. The markers illustrate the performance of other (non)linear classifiers for which the settings are determined using SVMs. The smallest markers indicate a training set size of 50, increasing via set sizes of 100, 150, 200, 250, 400, 500, 1000, and 1500 to the largest marker indicating a training set size of 2000 heartbeats. The dotted line indicates the line of no discrimination.

increasing size of the training set. The reason for the smaller impact on specificity than on sensitivity of the training set size can be explained by the fact that, for the data used in this study, the fetuses were resting approximately 25% more than that they were awake/moving. As a result, the various SVM classifiers were biased towards the accurate detection of fetal rest. In clinical practice, fetuses are also expected to rest more than to be awake and moving.

When comparing the nonlinear SVMs to the linear classifiers, it shows that both perform similar in detecting fetal movement. Exception is the mlp-kernel SVM for which the sensitivity/specificity is close to the line of no discrimination, indicating that this SVM is unsuitable for fetal movement detection. Upon use in clinical practice, specificity of the classification is more relevant than sensitivity. That is, the lack of fetal movement, especially when the fetus is awake, is an indication for fetal distress, whereas the presence of fetal movement does not automatically imply a good fetal condition. In addition, based on the finding that a small training set suffices for achieving a relatively high specificity in movement classification, it can be argued that a patient-invariable classifier should exist that can assess lack of fetal movement with a certainty of about 75%. Based on the results of the logistic regression, a specificity of 0.87 is achievable.

Based on these statements, it can be concluded that fetal VCG alignment can provide a valuable tool for assessing the fetal health condition. Due to its objectivity, it is expected to outperform movement counting by the mother, since this has been reported to be significantly susceptible to inter-patient variability [4]. Clinical decision-making based on the assessed movement (or lack thereof), however, requires additional studies. These studies need to assess whether absolute, relative and/or patient-specific cutoff values are needed for discriminating between 'still enough' and 'too little' fetal movements.

## REFERENCES

- [1] L. Sörnmo, "Vectorcardiographic loop alignment and morphologic beat-to-beat variability", *IEEE Trans Biomed Eng.*, vol. 45(12), 1998, pp. 1401–13.
- [2] M. Stridh and L. Sörnmo, "Spatiotemporal QRST cancellation techniques for analysis of atrial fibrillation", *IEEE Trans Biomed Eng.*, vol. 48(1), 2001, pp. 105–11.
- [3] J.V. Tveit, E. Saastad, B. Stray-Pedersen et al., "Reduction of late stillbirth with the introduction of fetal movement information and guidelines - a clinical quality improvement", *BMC Pregnancy Childbirth*, vol. 9(32), 2009.
- [4] L. Mangesi, G.J. Hofmeyr, "Fetal movement counting for assessment of fetal wellbeing", *Cochrane Database of Sys Rev.*, Issue 1, 2007.
- [5] M. Åström, E. Carro Santos, L. Sörnmo, P. Laguna, B. Wohlfart, "Vectorcardiographic loop alignment and the measurement of morphologic beat-to-beat variability in noisy signals", *IEEE Trans Biomed Eng.*, vol. 47(4), 2000, pp. 497–506.
- [6] F. Dellaert, "The Expectation Maximization Algorithm", *Tech rep.*, College of Computing, Georgia Institute of Technology, 2002.
- [7] R. Vullings, C.H.L. Peters, R.J. Sluijter et al. "Dynamic segmentation and linear prediction for maternal ECG removal in antenatal abdominal recordings", *Physiol. Meas.*, vol. 30, 2009, pp. 291–307.
- [8] R. Vullings, C.H.L. Peters, S.I. Mossavat, S.G. Oei, J.W.M. Bergmans, "Bayesian approach to patient-tailored vectorcardiography", *IEEE Trans Biomed Eng.*, vol. 57(3), 2010, pp. 586–95.